Electronic Supplementary Material (ESI) for Chemical Communications.

Electronic Supporting Information for

Nickel(II)-modified covalent-organic framework film for electrocatalytic oxidation of 5-hydroxymethylfufural (HMF)

Meng Cai, Sha Ding, Bradley Gibbons, Xiaozhou Yang, Matthew C. Kessinger and Amanda J. Morris*

Department of Chemistry, Virginia Polytechnic Institute and State University, 800 W. Campus Drive
Blacksburg, Virginia 24061, United States

*To whom correspondence should be addressed.

E-mail: ajmorris@vt.edu.

S1. Experimental methods

All chemicals and solvents were of analytical grade and used as obtained without further purification. FTO glass slides were first soaked in piranha solution for 20 min, and cleaned by sonicating in Alconox solution, water, ethanol, and acetone for 20 min each.

S1.1 Synthesis of triformylphloroglucinol (Tp)

Tp was synthesized by following a reported procedure.[1] To a three-neck round bottom flask, 15.098 g (108 mmol) of 1,3,5,7-tetraazaadamantane and 6.014 g (49 mmol) of phloroglucinol were added under nitrogen. 90 mL of trifluoroacetic acid was then added. The mixture was heated under reflux for 3 h. Then 150 mL of 3 M HCl was added slowly and the reaction solution was heated for 1 h. The solution obtained was filtered through Celite using a fritted funnel, and extracted with dichloromethane (DCM), dried over $MgSO_4$ and filtered. Consequently, the solvent was removed by rotary evaporation to yield a light-yellow powder.

S1.2 Synthesis of 5,5'-Diamino-2,2'-bipyridine (Bpy)

Bpy was prepared by a three-step reaction following previous studies with modification.[2, 3]

1-(2-Chloropyridine)-5-yl-2,5-dimethyl-1*H*-pyrrole: To a Dean-Stark apparatus, 1.0 g (7.8 mmol) of 5-amino-2-chloropyridine, 15 mg (0.08 mmol) of *p*-TsOH, and 1.1 mL (9.4 mmol) of 2,5-hexanedione were dissolved in 15 mL toluene. The reaction mixture was heated at 100 °C for 3 h. The dark brown solution was washed with saturated $NaHCO_3$ solution, water, and brine, dried over $MgSO_4$, and filtered. Solvent was removed by rotary evaporation to yield a brownish-yellow solid, which was used in next step without purification.

5,5'-Bis(2,5-dimethyl-1*H*-pyrrole)-2,2'-bipyridine: 0.74 g (1 mmol) of dibromobis(triphenylphosphane)nickel(II) bromide, 0.556 g (8.5 mmol) of zinc powder, and 1.28 g (5 mmol) of tetraethylammonium iodide were suspended in 20 mL of THF under nitrogen, and heated at 60 °C under stirring for 1 h. 1.04 g (5 mmol) of 1-(2-Chloropyridine)-5-yl-2,5-dimethyl-1*H*-pyrrole was dissolved in 10 mL of THF and added to the mixture slowly. The reaction solution was then stirred at 60 °C overnight. After cooling down to room temperature, 20 mL concentrated ammonia (25%), 15 mL of water, and 60 mL of DCM were added to the mixture that was stirred for 15 min. The organic layer was collected and the precipitate was filtered off. The aqueous layer was extracted with DCM (30 mL, 3 times), and the resulting organic phase was combined with previous organic layer. The solution was washed with water, brine, dried over $MgSO_4$ and concentrated by rotary evaporation. The crude was purified by column chromatography with DCM/hexanes (3:7) and then DCM/ethyl acetate (100:3) as eluent to give a light yellow solid.

5,5’-Diamino-2,2’-bipyridine (Bpy): 2.38 g (6.96 mmol) of 5,5’-bis(2,5-dimethyl-1*H*-pyrrole)-2,2’-bipyridine, 14.6 g (210 mmol) of hydroxylamine hydrochloride, and 8 mL of triethylamine were dissolved in a mixture of ethanol/water (50:20, 70 mL) and refluxed for 20 h. Then 14.6 g of hydroxylamine hydrochloride dissolving in 4 mL of triethylamine was added. The resulting mixture was further heated under reflux until TLC showed complete reaction. A clear yellow solution was obtained. After cooling down to room temperature, the reaction was quenched by pouring the mixture into 30 mL of ice-cold 3 M HCl. 100 mL of ethanol was then added and the mixture was stirred at 0 °C for 1 h. The precipitate was collected by filtration, and then dissolved in water. The pH was adjusted to 12 with 2 M NaOH. Finally, the precipitate was filtered, washed with water, and dried under vacuum. Bpy was obtained.

S1.3 Synthesis of TpBpy

TpBpy was prepared by an interfacial crystallization method based on previous report.[4] 14.5 mg (0.075 mmol) of Tp was dissolved in 100 mL of dichloromethane (DCM), and transferred to a 400 mL beaker. 60 mL of water was then carefully layered dropwise on top of the DCM solution. Afterwards, 20.8 mg (0.112 mmol) of Bpy and 45.8 mg (0.224 mmol) of *p*-toluenesulfonic acid (PTSA) were dissolved in 100 mL of water, and transferred dropwise to the water layer. The TpBpy film formed at the interface of the organic and aqueous layers after three days. After the film formation was finished, the aqueous layer was carefully removed using a pipet until minimum aqueous solution was left on top of TpBpy film. Then a clean FTO with the conductive side facing down was slowly lowered toward the film. Consequently, the film was transferred onto the FTO by “stamping”. The resulting TpBpy film on FTO was washed and soaked in water for one day to remove unreacted chemicals.

S1.4 Preparation of nickel-modified TpBpy (TpBpy-Ni) film

TpBpy-Ni was prepared by post-synthetic modification. 20 mg of $Ni(OAc)_2 \cdot 4H_2O$ was dissolved in 10 mL of methanol in a 6-dram vial. A TpBpy film was kept in the solution under stirring for 20 h. The resulting TpBpy-Ni film was rinsed and soaked in methanol for one day to remove loosely bound $Ni(OAc)_2 \cdot 4H_2O$.

S1.5 Material characterization

Scanning electron microscopy (SEM)

Scanning electron microscopy (SEM) images were collected using a Leo/Zeiss 1550 field-emission scanning electron microscope.

Transmission electron microscopy (TEM)

To prepare samples for TEM, ~5 mg of TpBpy-Ni film was scraped off from the substrate and dispersed in 1 mL methanol. The suspension was sonicated for 1 min and then 20 μL of the suspension was transferred to a lacey carbon grid. The grid was dried in air before use. TEM images were collected using JEOL 2100 transmission electron microscope.

Powder X-ray diffraction (PXRD)

PXRD patterns were obtained with a Rigaku Miniflex instrument (Cu Kα, $\lambda = 1.5418$ Å).

Inductively coupled plasma mass spectrometer (ICP-MS)

To determine the nickel content in TpBpy-Ni films, the modified films were digested in 70 % nitric acid and the solution was diluted 10 times with water. The resultant solution was tested using a Thermo Electron X-Series ICP-MS. The Ni loading was (33.3±11.8) mg m^{-2}.

N_2 adsorption/desorption isotherm

The N_2 adsorption/desorption were collected on a Quantachrome Autosorb-1, and the Brunauer-Emmett-Teller (BET) specific surface area was calculated.

X-ray photoelectron spectroscopy (XPS)

The XPS spectra were collected on a PHI 5000 Vera Probe III spectrometer using an aluminum anode X-ray source with photon energy of 1486.6 eV. Survey and elemental spectra were collected using a 100 µm beam size and 25 W, 15 kV source with a scan range of 1100 eV to 0 eV with a step size of 0.8 eV/step.

S1.6 Electrochemical measurements

Electrochemical measurements were carried out with an EC epsilon potentiostat (BASi) using a three-electrode setup. A TpBpy-Ni, a platinum mesh and a Ag/AgCl reference electrode were used as the working, counter and reference electrodes, respectively. DI water containing 0.1 M $LiClO_4$ and adjusted to pH 13 with NaOH was used as electrolyte. A certain amount of HMF was dissolved in solution for catalysis reaction. All potentials mentioned in this work were converted to the reversible hydrogen electrode (RHE) according to the following equation:

$$E_{RHE} = E_{Ag/AgCl} + 0.059\ V \times pH + E^{0}_{Ag/AgCl}$$

and $$E^{0}_{Ag/AgCl} = 0.1976\ V\ vs.\ NHE\ at\ 25℃$$

S1.7 High-performance liquid chromatography (HPLC) analysis

The HPLC analysis was performed on a Waters HPLC with 2487 absorbance detector, 1525 binary pump and 717 autosampler. The reverse-phase C18 column used was purchased from Phenomenex (5 µm ODS2 80 Å, LC Column 250 x 4.6 mm). The crude was separated using a linear gradient of acetonitrile/water (20 mM ammonium acetate, pH = 5 adjusted with acetic acid) from 5:95 to

95:5 (v:v) over 12.5 mins, 1mL min^{-1}. Calibration curves of HMF, HMFCA, DFF, FFCA, and FDCA were generated from a series of standard solutions (prepared in 50:50 acetonitrile/water) with known concentrations (Figure S5.5). The experiments were repeated three times and the average values were used for generating calibration curves. For analysis of catalysis reaction, 50 μL of reaction solution was removed from the electrochemical cell and diluted with 450 μL of 50:50 acetonitrile/water.

S2. Supporting figures

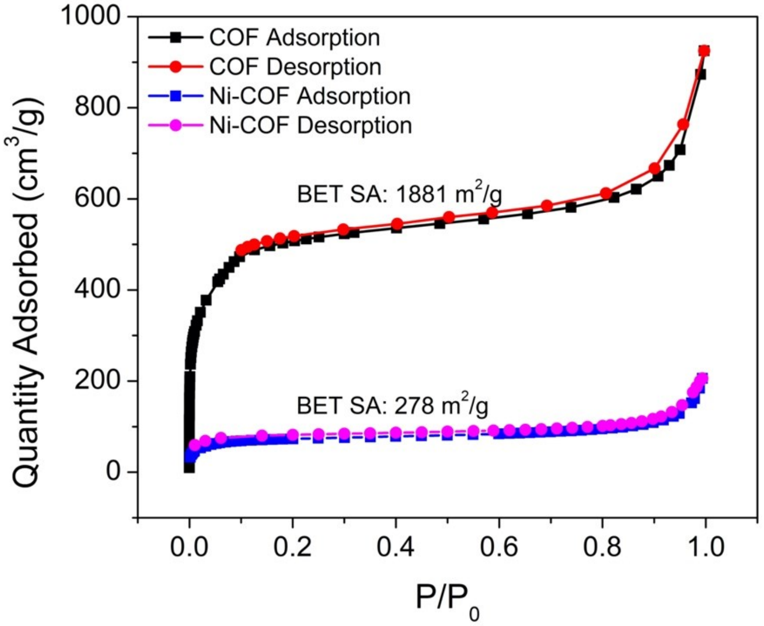

Figure S1. N_2 sorption isotherms of unmodified TpBpy (black/red) and Ni-TpBpy (blue/pink).

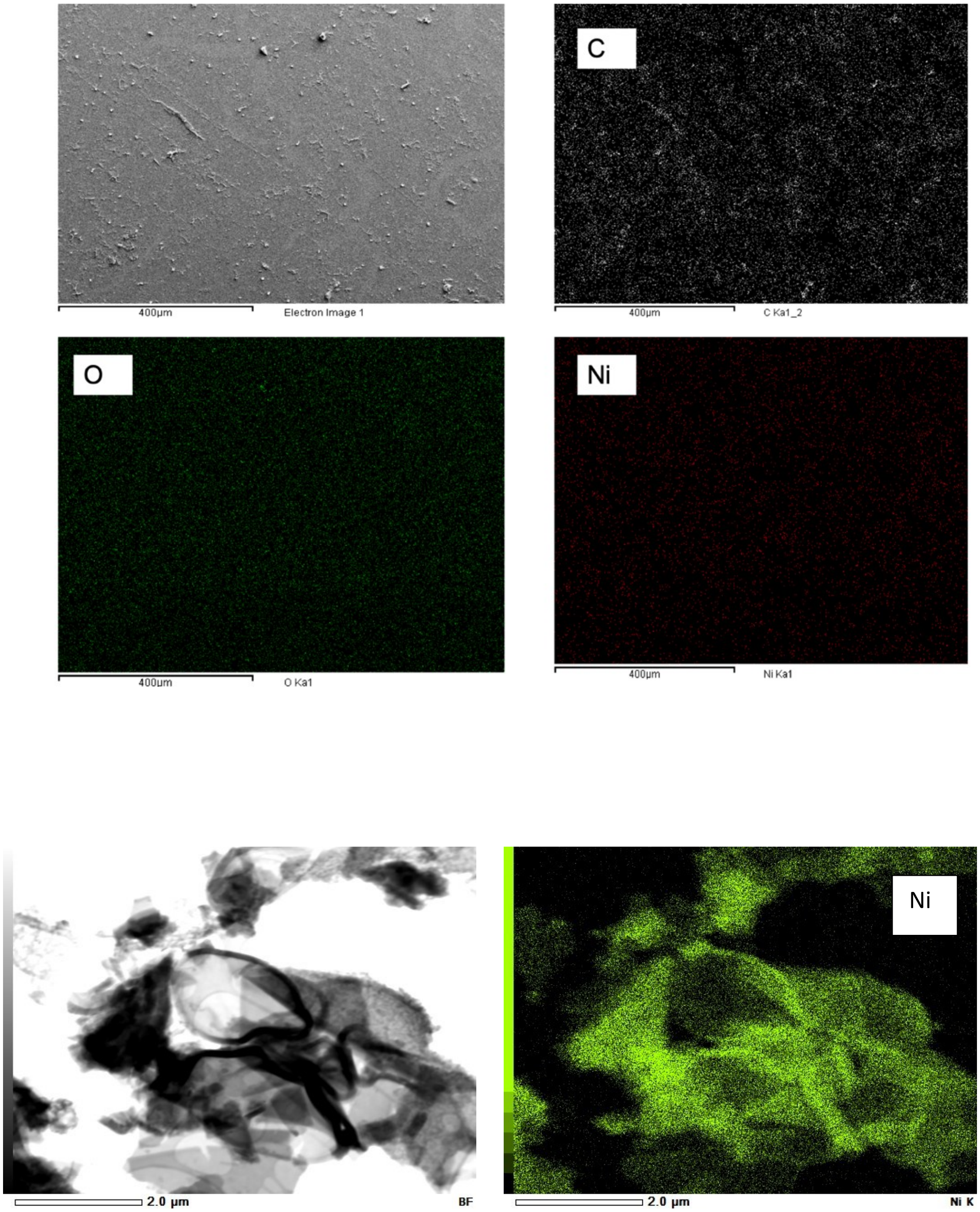

Figure S2 SEM EDS mapping (top) and TEM (bottom) EDS mapping of TpBpy-Ni film.

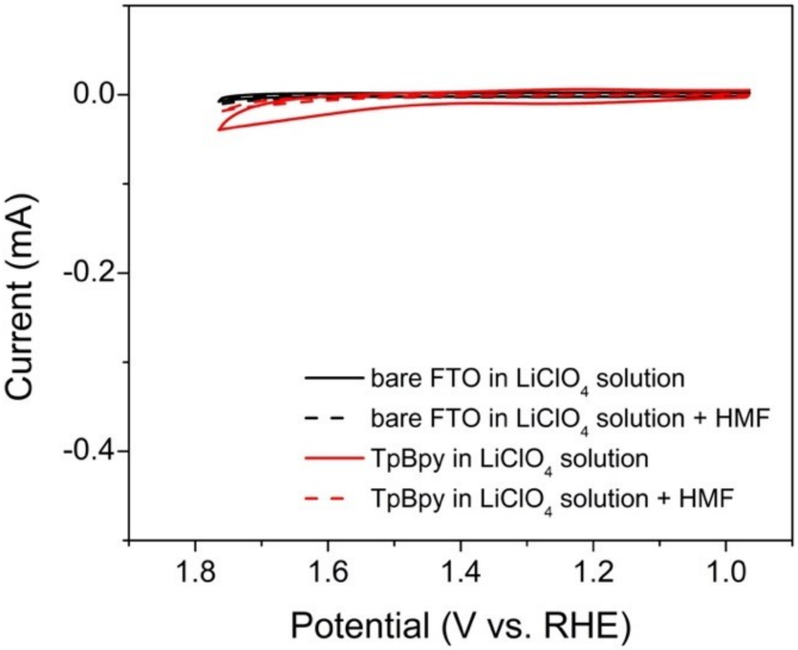

Figure S3 CVs of a bare FTO (black) and unmodified TpBpy@FTO (red) in the absence (solid line) and presence (dotted line) of HMF, in 0.1 M $LiClO_4$ solution.

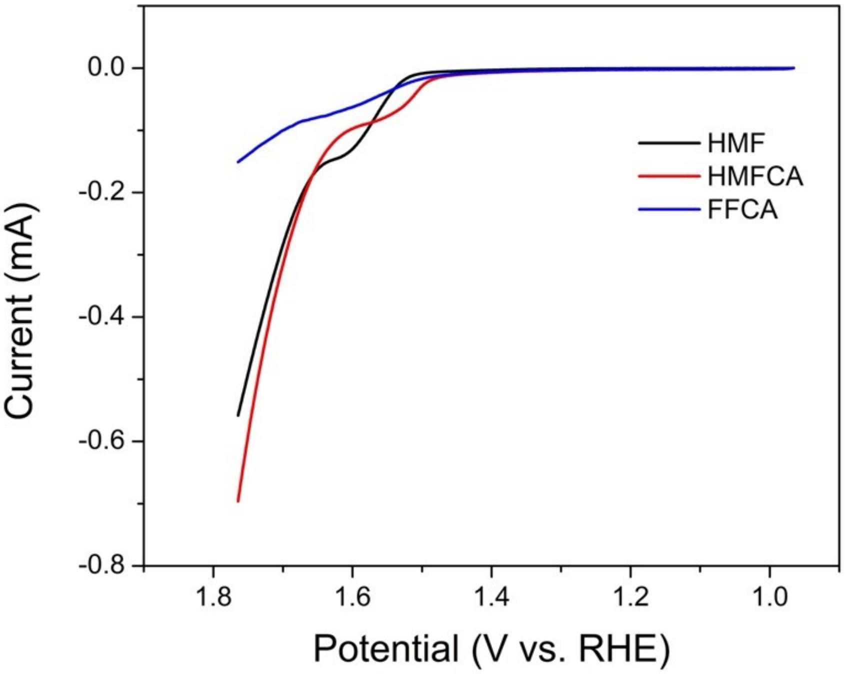

Figure S4 LSVs of TpBpy-Ni@FTO in the presence of 5 mM HMF (black), HMFCA (red), or FFCA (blue) in 0.1 M LiClO4 solution (pH = 13).

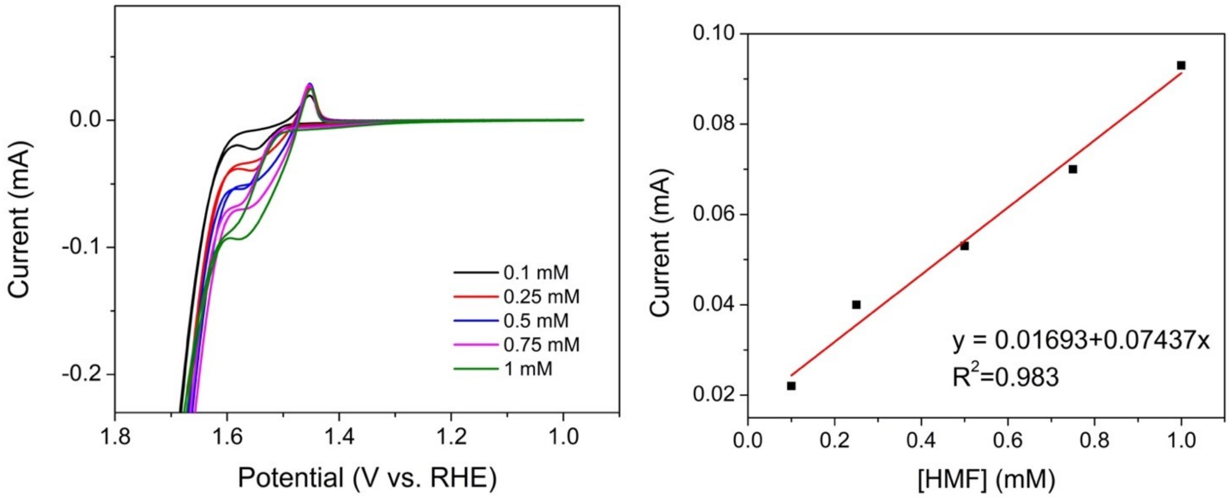

Figure S5 a) CVs of TpBpy-Ni@FTO in the presence of 0.1–1 mM HMF. b) Current vs. HMF concentration.

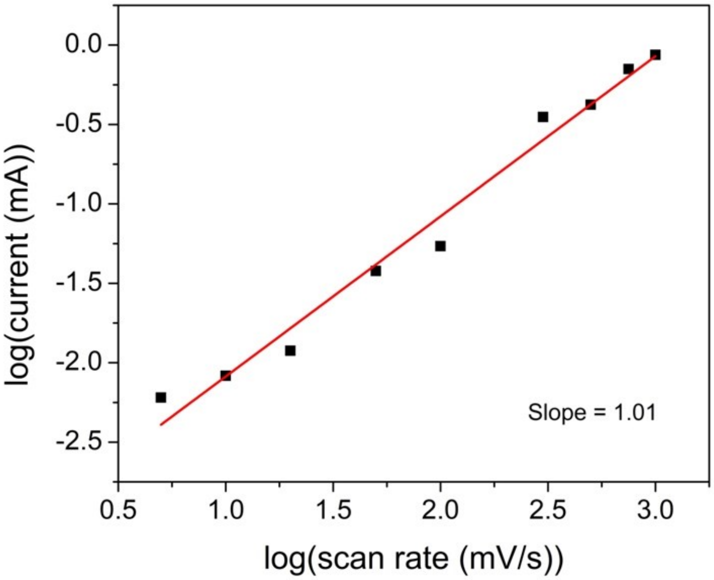

Figure S6 The plot of logarithm of peak currents vs. logarithm of scan rates.

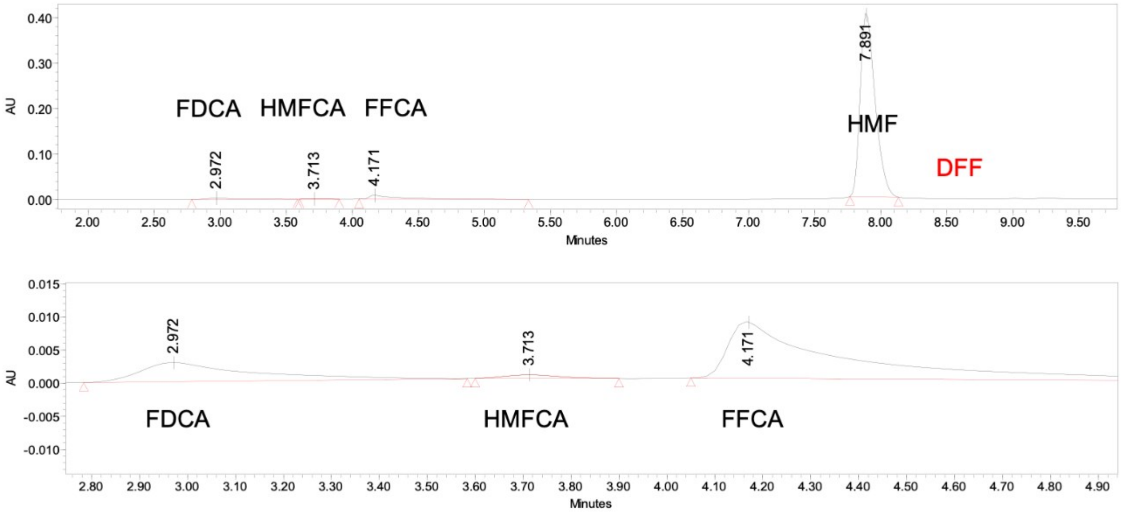

Figure S7 Chromatograms of HMF oxidation after passing 2 C.

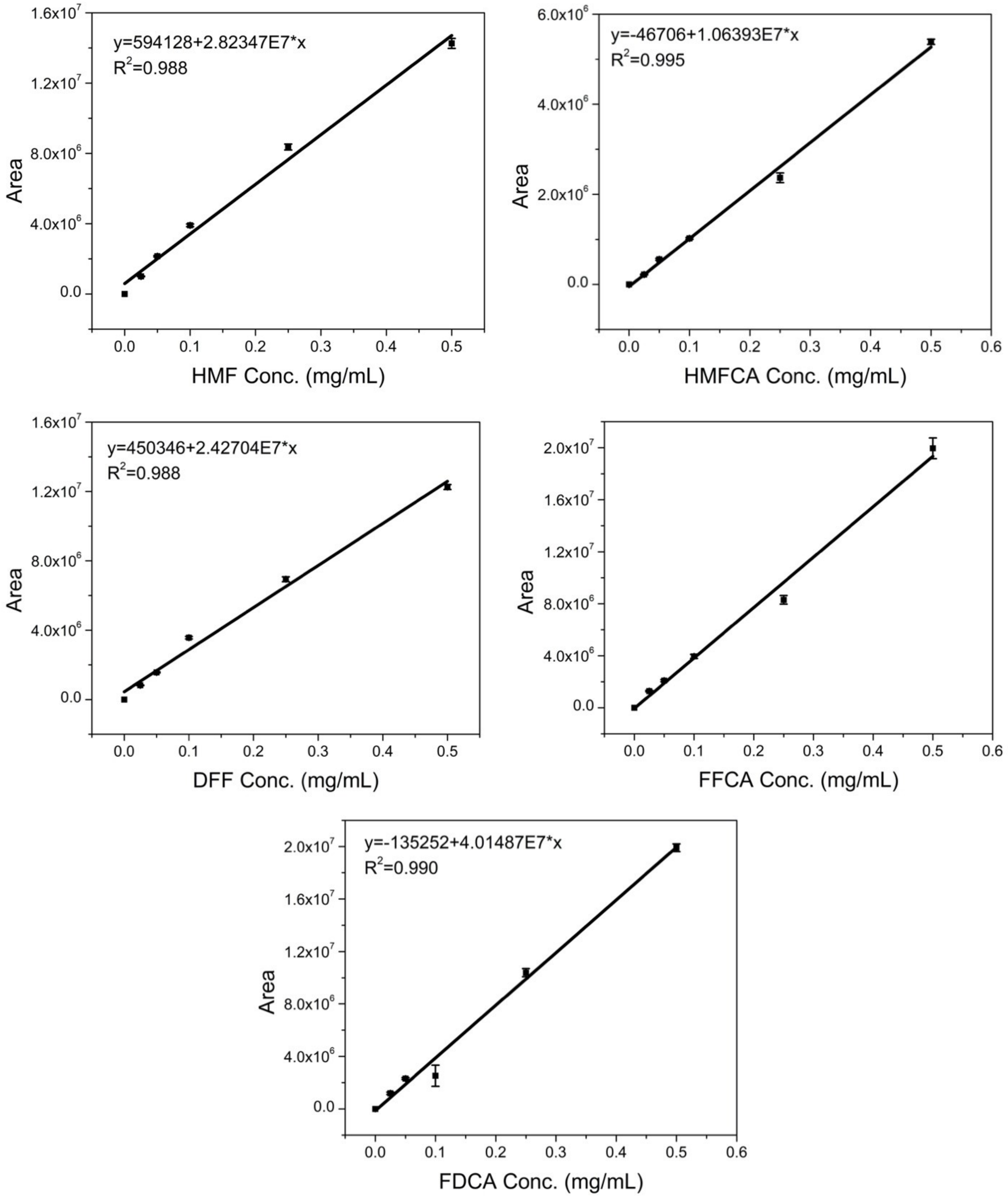

Figure S8 Calibration curves for HMF, HMFCA, DFF, FFCA, and FDCA.

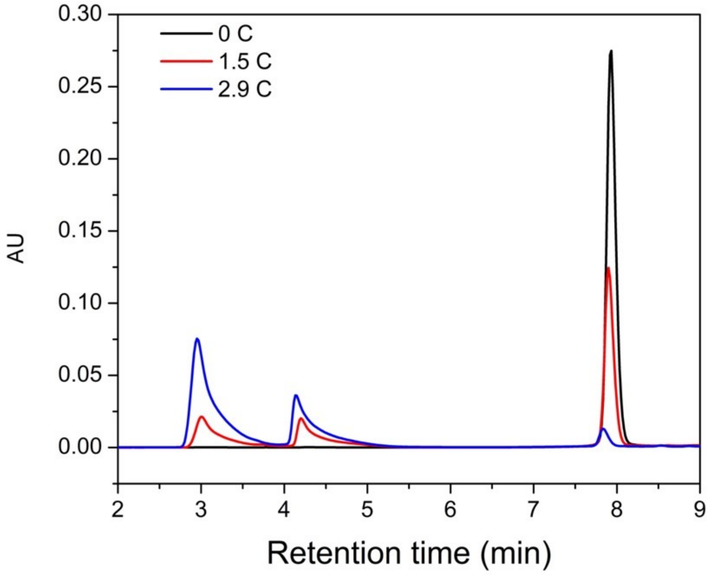

Figure S9 HPLC chromatograms collected after passing 0, 1.5, and 2.9 C of charge during controlled potential electrolysis at 1.55 V vs. RHE.

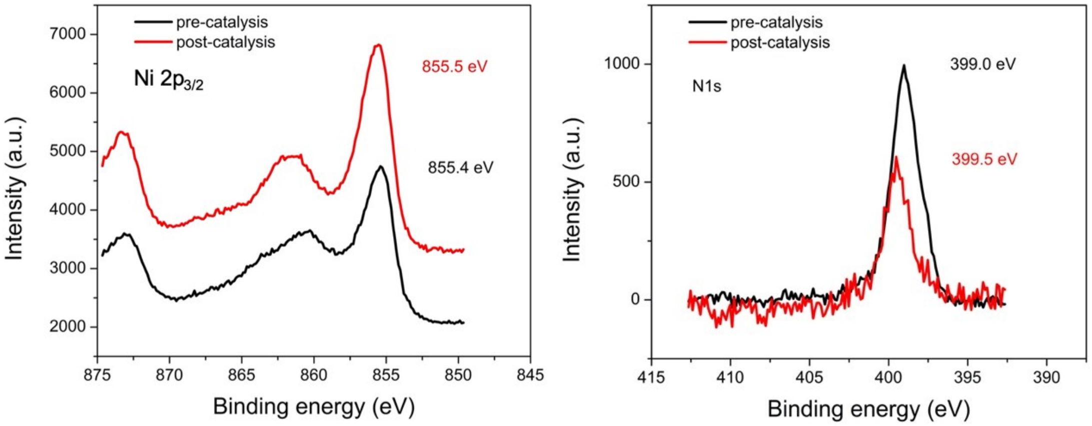

Figure S10 XPS spectra of Ni2p3/2 and N1s peaks of TpBpy-Ni@FTO pre-catalysis (black line) and post-catalysis (red line).

S3. Supporting tables

Table S1. Average values and standard deviations for HMF conversion

Charge	HMF conversion (%)	FDCA yield (%)	HMFCA yield (%)	FFCA yield (%)	DFF yield (%)
0	0	0	0	0	0
0.5	50.4 (±5.2)	23.0 (±1.8)	14.1(±1.4)	13.3 (±3.0)	0
1	53.5 (±2.3)	23.2 (±0.3)	16.2 (±1.5)	14.1 (±4.7)	0
1.5	83.4 (±0.6)	43.5 (±2.9)	10.7 (±1.8)	29.2 (±3.7)	0
2	91.1 (±0.5)	54.1 (±7.1)	9.5 (±0.9)	35.5 (±2.0)	0
2.5	94.6 (±1.0)	55.2 (±0.8)	8.4 (±1.0)	31.1 (±0.5)	0
2.9	96.5 (±0.3)	58.1 (±1.9)	0.1 (±0.4)	34.2 (±0.2)	0

Table S2. Comparison of current work and some previous work for HMF oxidation

Catalyst	Electrode	Conditions	HMF conversion	Product yields	Refs
thiophene-containing covalent triazine framework (CTF-Th)	mesoporous silica (SBA-15)	water, 460nm blue light	57%	100% DFF	[5]
NiFe LDH	carbon paper	1 M KOH sol.	99%	98% FDCA	[6]
t-Ni1Co1-MOF	Ni foam	1 M KOH sol.	~100%	96% FDCA	[7]
Pt	Pt foil	pH 10 NaOH sol.	29%	7.69% DFF	[8]
Ni-TpBpy	FTO slide	0.1 M NaOH sol.	96%	58% FDCA 34% FFCA	This work

S4. Calculations

The theoretical charge that is needed for a complete HMF oxidation is calculated based on the oxidation reaction:

$HMF + 6OH^{-} \rightarrow FDCA + 4H_2O + 6e^{-}$

For 10 mL of 0.5 mM HMF solution, the total charge needed is:

$$0.01\ L \times 0.0005 \frac{mol}{L} \times 96485 \frac{C}{mol} \times 6 = 2.9\ C$$

The HMF conversion and product yield were calculated following:

$$HMF\ conversion\ (\%) = \frac{mol\ of\ HMF\ consumed}{mol\ of\ initial\ HMF} \times 100$$

$$yield\ of\ product (\%) = \frac{mol\ of\ product\ formed}{mol\ of\ initial\ HMF} \times 100$$

S5. References

1 J. H. Chong, M. Sauer, B. O. Patrick and M. J. MacLachlan, *Org. Lett.*, 2003, **5**, 3823-3826.
2 M. Albrecht, I. Janser, A. Lützen, M. Hapke, R. Fröhlich and P. Weis, *Chem. Eur. J.*, 2005, **11**, 5742-5748.
3 Q. Sun, B. Aguila, J. Perman, N. Nguyen and S. Ma, *Journal of the American Chemical Society*, 2016, **138**, 15790-15796.
4 K. Dey, M. Pal, K. C. Rout, S. Kunjattu H, A. Das, R. Mukherjee, U. K. Kharul and R. J. J. o. t. A. C. S. Banerjee, 2017, **139**, 13083-13091.
5 C. Ayed, W. Huang, G. Kizilsavas, K. Landfester and K. A. I. Zhang, *ChemPhotoChem*, 2020, **4**, 571-576.
6 W.-J. Liu, L. Dang, Z. Xu, H.-Q. Yu, S. Jin and G. W. Huber, *ACS Catal.*, 2018, **8**, 5533-5541.
7 X. Deng, M. Li, Y. Fan, L. Wang, X.-Z. Fu and J.-L. Luo, *Appl. Catal. B Environ.*, 2020, **278**, 119339.
8 A. S. Varela, M. Kroschel, N. D. Leonard, W. Ju, J. Steinberg, A. Bagger, J. Rossmeisl and P. Strasser, *ACS Energy Lett.*, 2018, **3**, 812-817.